

OUTLIER EXPOSURE WITH CONFIDENCE CONTROL FOR OUT-OF-DISTRIBUTION DETECTION

Aristotelis-Angelos Papadopoulos & Mohammad Reza Rajati & Nazim Shaikh & Jiamian Wang
 University of Southern California
 Los Angeles, CA 90089, USA
 {aristop, rajati, nshaikh, jiamianw}@usc.edu

ABSTRACT

Deep neural networks have achieved great success in classification tasks during the last years. However, one major problem to the path towards artificial intelligence is the inability of neural networks to accurately detect samples from novel class distributions and therefore, most of the existent classification algorithms assume that all classes are known prior to the training stage. In this work, we propose a methodology for training a neural network that allows it to efficiently detect out-of-distribution (OOD) examples without compromising much of its classification accuracy on the test examples from known classes. Based on the Outlier Exposure (OE) technique, we propose a novel loss function that gives rise to a novel method, Outlier Exposure with Confidence Control (OECC), which achieves superior results in out-of-distribution detection with OE both on image and text classification tasks without requiring access to OOD samples. Additionally, we experimentally show that the combination of OECC with state-of-the-art post-training OOD detection methods further improves their performance in the OOD detection task, demonstrating the potential of combining training and post-training methods for OOD detection.¹

1 INTRODUCTION

Modern neural networks have recently achieved superior results in classification problems (Krizhevsky et al., 2012; He et al., 2016). However, most of the classification algorithms proposed so far make the assumption that data generated from all the class conditional distributions are available during training time i.e., they make the closed-world assumption. In an open world environment (Bendale & Boult, 2015), where examples from novel class distributions might appear during test time, it is necessary to build classifiers that are able to detect OOD examples while having high classification accuracy on known class distributions.

It is generally known that deep neural networks can make predictions for out-of-distribution (OOD) examples with high confidence (Nguyen et al., 2015). High confidence predictions are undesirable since they consist a symptom of overfitting (Szegedy et al., 2015). They also make the calibration of neural networks difficult. Guo et al. (2017) observed that modern neural networks are miscalibrated since their average confidence is usually much higher than their accuracy.

A simple yet effective method to address the problem of the inability of neural networks to detect OOD examples is to train them so that they make highly uncertain predictions for examples generated by novel class distributions. In order to achieve that, Lee et al. (2018a) defined a loss function based on the Kullback-Leibler (KL) divergence to minimize the distance between the output distribution given by softmax and the uniform distribution for samples generated by a GAN (Goodfellow et al., 2014). Using a similar loss function, Hendrycks et al. (2019) showed that the technique of Outlier Exposure (OE) that draws anomalies from a real and diverse dataset can outperform the GAN framework for OOD detection.

Using the OE technique, our main contribution is threefold:

¹Our code is publicly available at <https://github.com/nazim1021/OOD-detection-using-OECC>.

- We propose a novel method, Outlier Exposure with Confidence Control (OECC), consisting of two regularization terms. The first regularization term minimizes the l_1 norm between the output distribution given by softmax and the uniform distribution, which constitutes a distance metric between the two distributions (Deza & Deza, 2009). The second regularization term minimizes the Euclidean distance between the training accuracy of a DNN and its average confidence in its predictions on the training set.
- We experimentally show that OECC achieves superior results in OOD detection with OE without requiring access to OOD samples. Additionally, similar to Hendrycks et al. (2019) and in contrast with many other state-of-the-art OOD detection methods (Lee et al., 2018b; Sastry & Oore, 2019; Liang et al., 2018), we show that OECC can be applied to both image and text classification tasks.
- We experimentally show that OECC can be combined with state-of-the-art post-training methods for OOD detection like the Mahalanobis Detector (MD) (Lee et al., 2018b) and the Gramian Matrices method (GM) (Sastry & Oore, 2019). The experimental results demonstrate that the resulting combination achieves superior results in the OOD detection task, demonstrating the potential of combining training and post-training methods for OOD detection in the future research efforts.

2 RELATED WORK

Yu et al. (2017) used the GAN framework (Goodfellow et al., 2014) to generate negative instances of seen classes by finding data points that are close to the training instances but are classified as fake by the discriminator. Then, they used those samples in order to train SVM classifiers to detect examples from unseen classes. Similarly, Klier & Fleishman (2018) used a multi-class GAN framework in order to produce a generator that generates a mixture of nominal data and novel data and a discriminator that performs simultaneous classification and novelty detection.

Hendrycks & Gimpel (2017) proposed a baseline for detecting misclassified and out-of-distribution examples based on their observation that the prediction probability of out-of-distribution examples tends to be lower than the prediction probability for correct examples. A single-parameter variant of Platt scaling (Platt, 1999), temperature scaling, was proposed by Guo et al. (2017) for calibration of modern neural networks. For image data, based on the idea of Hendrycks & Gimpel (2017), it was observed that simultaneous use of temperature scaling and small perturbations at the input can push the softmax scores of in- and out-of-distribution images further apart from each other, making the OOD images distinguishable (Liang et al., 2018). Lee et al. (2018a) generated GAN examples and forced the DNN to have lower confidence in predicting the classes for those examples while in Hendrycks et al. (2019), the GAN samples were substituted with a real and diverse dataset using the technique of OE. Similar works (Malinin & Gales, 2018; Bevandić et al., 2018) also force the model to make uncertain predictions for OOD examples. Using an ensemble of classifiers, Lakshminarayanan et al. (2017) showed that their method was able to express higher uncertainty in OOD examples. Liu et al. (2018) provided theoretical guarantees for detecting OOD examples under the assumption that an upper bound of the fraction of OOD examples is available.

Under the assumption that the pre-trained features of a softmax neural classifier can be fitted well by a class-conditional Gaussian distribution, one can define a confidence score using the Mahalanobis distance that can efficiently detect abnormal test samples (Lee et al., 2018b). Sastry & Oore (2019) proposed the use of higher order Gram matrices to compute pairwise feature correlations between the channels of each layer of a DNN. Both approaches (Lee et al., 2018b; Sastry & Oore, 2019) are post-training methods for OOD detection.

Recently, there is also a growing interest in applying machine learning in a self-supervised manner for the OOD detection task. Hendrycks et al. (2019b) combined different self-supervised geometric translation prediction tasks in one model, using multiple auxiliary heads. They showed that their method performs well on detecting outliers which are close to the in-distribution data. Mohseni et al. (2020) proposed using one auxiliary head in a self-supervised manner to learn generalizable OOD features.

3 OUTLIER EXPOSURE WITH CONFIDENCE CONTROL (OECC)

We consider the multi-class classification problem under the open-world assumption (Bendale & Boult, 2015), where samples from some classes are not available during training. Our task is to design deep neural network classifiers that can achieve high accuracy on examples generated by a learned probability distribution called D_{in} while at the same time, they can effectively detect examples generated by a different probability distribution called D_{out} during the test phase. The examples generated by D_{in} are called in-distribution while the examples generated by D_{out} are called out-of-distribution (OOD). Adopting the idea of Outlier Exposure (OE) proposed by Hendrycks et al. (2019), we train the neural network using training examples sampled from D_{in} and D_{out}^{OE} . During the test phase, we evaluate the OOD detection capability of the neural network using examples sampled from D_{out}^{test} , where D_{out}^{OE} and D_{out}^{test} are disjoint.

In previous works (Lee et al., 2018a; Hendrycks et al., 2019), the KL divergence metric was used in order to minimize the distance between the output distribution produced by softmax for the OOD examples and the uniform distribution. However, it is generally known that KL divergence does not satisfy the symmetry and the triangular inequality properties as required by a distance metric (Deza & Deza, 2009). In our work, we choose to minimize the l_1 norm between the two distributions which has shown great success in machine learning applications.

Viewing the knowledge of a model as the class conditional distribution it produces over outputs given an input (Hinton et al., 2015), the entropy of this conditional distribution can be used as a regularization method that penalizes confident predictions of a neural network (Pereyra et al., 2017). In our approach, instead of penalizing the confident predictions of posterior probabilities yielded by a neural network, we force it to make predictions for examples generated by D_{in} with an average confidence close to its training accuracy. In such a manner, not only do we make the neural network avoid making overconfident predictions, but we also take into consideration its calibration (Guo et al., 2017).

Let us consider a classification model that can be represented by a parametrized function f_{θ} , where θ stands for the vector of parameters in f_{θ} . Without loss of generality, assume that the cross-entropy loss function is used during training. We propose the following constrained optimization problem for finding θ :

$$\begin{aligned} & \underset{\theta}{\text{minimize}} \quad \mathbb{E}_{(x,y) \sim D_{in}} [\mathcal{L}_{CE}(f_{\theta}(x), y)] \\ & \text{subject to} \quad \mathbb{E}_{x \sim D_{in}} \left[\max_{l=1, \dots, K} \left(\frac{e^{z_l}}{\sum_{j=1}^K e^{z_j}} \right) \right] = A_{tr} \\ & \quad \max_{l=1, \dots, K} \left(\frac{e^{z_l}}{\sum_{j=1}^K e^{z_j}} \right) = \frac{1}{K}, \quad \forall x^{(i)} \sim D_{out}^{OE} \end{aligned} \quad (1)$$

where \mathcal{L}_{CE} is the cross-entropy loss function and K is the number of classes available in D_{in} . Even though the constrained optimization problem (1) can be used for training various classification models, for clarity we limit our discussion to deep neural networks. Let \mathbf{z} denote the vector representation of the example $x^{(i)}$ in the feature space produced by the last layer of the deep neural network (DNN) and let A_{tr} be the training accuracy of the DNN. Observe that the optimization problem (1) minimizes the cross entropy loss function subject to two additional constraints. The first constraint forces the average maximum prediction probabilities calculated by the softmax layer towards the training accuracy of the DNN for examples sampled from D_{in} , while the second constraint forces the maximum probability calculated by the softmax layer towards $\frac{1}{K}$ for all examples sampled from the probability distribution D_{out}^{OE} . In other words, the first constraint makes the DNN predict examples from known classes with an average confidence close to its training accuracy, while the second constraint forces the DNN to be highly uncertain for examples of classes it has never seen before by producing a uniform distribution at the output for examples sampled from the probability distribution D_{out}^{OE} . It is also worth noting that the first constraint of (1) uses the training accuracy of the neural network A_{tr} which is not available in general. To handle this issue, one can train a neural network by only minimizing the cross-entropy loss function for a few number of epochs in order to estimate A_{tr} and then fine-tune it using (1).

Because solving the nonconvex constrained optimization problem described by (1) is extremely difficult, let us introduce Lagrange multipliers (Boyd & Vandenberghe, 2004) and convert (1) into the following unconstrained optimization problem:

$$\begin{aligned} \underset{\theta}{\text{minimize}} \quad & \mathbb{E}_{(x,y) \sim D_{in}} [\mathcal{L}_{CE}(f_{\theta}(x), y)] \\ & + \lambda_1 \left(A_{tr} - \mathbb{E}_{x \sim D_{in}} \left[\max_{l=1, \dots, K} \left(\frac{e^{z_l}}{\sum_{j=1}^K e^{z_j}} \right) \right] \right) \\ & + \lambda_2 \sum_{x^{(i)} \sim D_{out}^{OE}} \left(\frac{1}{K} - \max_{l=1, \dots, K} \left(\frac{e^{z_l}}{\sum_{j=1}^K e^{z_j}} \right) \right) \end{aligned} \quad (2)$$

where it is worth mentioning that in (2), we used only one Lagrange multiplier for the second set of constraints in (1) instead of using one for each constraint in order to avoid introducing a large number of hyperparameters to our loss function. This modification is a special case where we consider the Lagrange multiplier λ_2 to be common for each individual constraint involving a different $x^{(i)} \sim D_{out}^{OE}$. Note also that according to the original Lagrangian theory, one should optimize the objective function of (2) both with respect to θ , λ_1 and λ_2 but as it commonly happens in machine learning applications, we approximate the original problem by calculating appropriate values for λ_1 and λ_2 through a validation technique (Hastie et al., 2001).

After converting the constrained optimization problem (1) into an unconstrained optimization problem as described by (2), it was observed in the simulation experiments that at each training epoch, the maximum prediction probability produced by softmax for each example drawn from D_{out}^{OE} changes, introducing difficulties in making the DNN produce a uniform distribution at the output for those examples. For instance, assume that we have a K -class classifier with $K = 3$ and at epoch t_n , the maximum prediction probability produced by softmax for an example $x^{(i)} \sim D_{out}^{OE}$ corresponds to the second class. Then, the last term of (2) will push the prediction probability of example $x^{(i)}$ for the second class towards $\frac{1}{3}$ while concurrently increasing the prediction probabilities for either the first class or the third class or both. At the next epoch t_{n+1} , it is possible that the prediction probability for either the first class or the third class becomes the maximum among the three and hence, the last term of (2) will push that one towards $\frac{1}{3}$ by possibly increasing again the prediction probability for the second class. It becomes obvious that this process introduces difficulties in making the DNN produce a uniform distribution at the output for examples sampled from D_{out}^{OE} . However, this issue can be resolved by concurrently pushing all the prediction probabilities produced by the softmax layer for examples drawn from D_{out}^{OE} towards $\frac{1}{K}$.

Additionally, in order to prevent the second and the third term of (2) from taking negative values during training, let us convert (2) into the following:

$$\begin{aligned} \underset{\theta}{\text{minimize}} \quad & \mathbb{E}_{(x,y) \sim D_{in}} [\mathcal{L}_{CE}(f_{\theta}(x), y)] \\ & + \lambda_1 \left(A_{tr} - \mathbb{E}_{x \sim D_{in}} \left[\max_{l=1, \dots, K} \left(\frac{e^{z_l}}{\sum_{j=1}^K e^{z_j}} \right) \right] \right)^2 \\ & + \lambda_2 \sum_{x^{(i)} \sim D_{out}^{OE}} \sum_{l=1}^K \left| \frac{1}{K} - \frac{e^{z_l}}{\sum_{j=1}^K e^{z_j}} \right| \end{aligned} \quad (3)$$

The second term of the the loss function described by (3) minimizes the squared distance between the training accuracy of the DNN and the average confidence in its predictions for examples drawn from D_{in} . Additionally, the third term of (3) minimizes the l_1 norm between the uniform distribution and the distribution produced by the softmax layer for the examples drawn from D_{out}^{OE} . We call the methodology of training a DNN with the loss function described by (3) Outlier Exposure with Confidence Control (OECC).

While converting the unconstrained optimization problem (2) into (3), one could use several combinations of norms to minimize. However, we found that minimizing the squared distance between the training accuracy of the DNN and the average confidence in its predictions for examples drawn from D_{in} and the l_1 norm between the uniform distribution and the distribution produced by the softmax

layer for the examples drawn from D_{out}^{OE} works best. This is because l_1 norm uniformly attracts all the prediction probabilities produced by softmax to the desired value $\frac{1}{K}$, better contributing to producing a uniform distribution at the output of the DNN for the examples drawn from D_{out}^{OE} . On the other hand, minimizing the squared distance between the training accuracy of the DNN and the average confidence in its predictions for examples drawn from D_{in} emphasizes more on attracting the maximum softmax probabilities that are further away from the training accuracy of the DNN, making the neural network better detect in- and out-of-distribution examples at the low softmax probability levels.

4 EXPERIMENTS

During the experiments, we observed that if we start training the DNN with a relatively high value of λ_1 , the learning process might slow down since we constantly force the neural network to make predictions with an average confidence close to its training accuracy, which is initially low mainly due to the random weight initialization. Therefore, it is recommended to split the training of the algorithm into two stages where in the first stage, we train the DNN using only the cross entropy loss function until it reaches the desired level of accuracy A_{tr} and then using a fixed A_{tr} , we fine-tune it using the OECC method.²

4.1 COMPARISON WITH STATE-OF-THE-ART IN OE

The experimental setting at this paper is as follows. We draw samples from D_{in} and we train the DNN until it reaches the desired level of accuracy A_{tr} . Then, drawing samples from D_{out}^{OE} , we fine-tune it using the OECC method given by (3). During the test phase, we evaluate the OOD detection capability of the DNN using examples from D_{out}^{test} which is disjoint from D_{out}^{OE} . We demonstrate the effectiveness of our method in both image and text classification tasks by comparing it with the previous OOD detection with OE method proposed by Hendrycks et al. (2019), which is a state-of-the-art method in OE. A part of our experiments was based on the publicly available code of Hendrycks et al. (2019).

4.1.1 EVALUATION METRICS

Our OOD detection method belongs to the class of Maximum Softmax Probability (MSP) detectors (Hendrycks & Gimpel, 2017) and therefore, we adopt the evaluation metrics used in Hendrycks et al. (2019). Defining the OOD examples as the positive class and the in-distribution examples as the negative class, the performance metrics associated with OOD detection are the following:

- False Positive Rate at $N\%$ True Positive Rate (FPR_N): This performance metric (Balntas et al., 2016; Kumar et al., 2016) measures the capability of an OOD detector when the maximum softmax probability threshold is set to a predefined value. More specifically, assuming $N\%$ of OOD examples need to be detected during the test phase, we calculate a threshold in the softmax probability space and given that threshold, we measure the false positive rate, i.e. the ratio of in-distribution examples that are incorrectly classified as OOD.
- Area Under the Receiver Operating Characteristic curve (AUROC): In the out-of-distribution detection task, the ROC curve (Davis & Goadrich, 2006) summarizes the performance of an OOD detection method for varying threshold values.
- Area Under the Precision-Recall curve (AUPR): The AUPR (Manning & Schütze, 1999) is an important measure when there exists a class-imbalance between OOD and in-distribution examples in a dataset. As in Hendrycks et al. (2019), in our experiments, the ratio of OOD and in-distribution test examples is 1:5.

4.1.2 IMAGE CLASSIFICATION EXPERIMENTS

Results. The results of the image classification experiments are shown in Table 1. In Figure 1, as an example, we plot the histogram of softmax probabilities using CIFAR-10 as D_{in} and Places365 as D_{out}^{test} . The detailed description of the image datasets used in the image OOD detection experiments is presented in Appendix A.2.

²Our code is publicly available at <https://github.com/nazim1021/OOD-detection-using-OECC>.

D_{in}	FPR95↓		AUROC↑		AUPR↑	
	+OE	OECC	+OE	OECC	+OE	OECC
SVHN	0.10	0.03	99.98	99.99	99.83	99.55
CIFAR-10	9.50	6.56	97.81	98.40	90.48	93.08
CIFAR-100	38.50	28.89	87.89	91.80	58.15	71.50

Table 1: Image OOD example detection for the maximum softmax probability (MSP) baseline detector after fine-tuning with OE (Hendrycks et al., 2019) versus fine-tuning with OECC given by (3). All results are percentages and averaged over 10 runs and over 8 OOD datasets. Detailed experimental results are shown in Appendix A.1.

Network Architecture and Training Details. Similar to Hendrycks et al. (2019), for CIFAR-10 and CIFAR-100 experiments, we used 40-2 Wide Residual Networks (WRNs) proposed by Zagoruyko & Komodakis (2016). We initially trained the WRN for 100 epochs using a cosine learning rate (Loshchilov & Hutter, 2017) with an initial value 0.1, a dropout rate of 0.3 and a batch size of 128. As in Hendrycks et al. (2019), we also used Nesterov momentum and l_2 weight regularization with a decay factor of 0.0005. For CIFAR-10, we fine-tuned the network for 15 epochs with the OECC method described by (3) using a learning rate of 0.001, while for the CIFAR-100 the corresponding number of epochs was 20. For the SVHN experiments, we trained 16-4 WRNs using a learning rate of 0.01, a dropout rate of 0.4 and a batch size of 128. We then fine-tuned the network for 5 epochs using a learning rate of 0.001. During fine-tuning, the 80 Million Tiny Images dataset was used as D_{out}^{OE} . Note that D_{out}^{OE} and D_{out}^{test} are disjoint. The values of the hyperparameters λ_1 and λ_2 were chosen in the range [0.03, 0.09] using a separate validation dataset D_{out}^{val} similar to Hendrycks et al. (2019). Note that D_{out}^{val} and D_{out}^{test} are disjoint. The data used for validation are presented in Appendix A.3.

Contribution of each regularization term. To demonstrate the effect of each regularization term of the OECC method described by (3) in the OOD detection task, we ran some additional image classification experiments which are presented in Table 2. For these added each regularization term to the loss function described by (3) and we measured its effect both in the OOD detection evaluation metrics as well as in the accuracy of the DNN on the test images of D_{in} . The results of these experiments validate that the combination of the two regularization terms of (3) not only improves the OOD detection performance of the DNN but also improves its accuracy on the test examples of D_{in} compared to the case where $\lambda_1 = 0$. Table 2 also demonstrates that our method can significantly improve the OOD detection performance of the DNN compared to the case where only the cross-entropy loss is minimized at the expense of only an insignificant degradation in the test accuracy of the DNN on examples generated by D_{in} .

D_{in}	λ_1	λ_2	FPR95↓	AUROC↑	AUPR↑	Test Accuracy(D_{in})
CIFAR-10	-	-	34.94	89.27	59.16	94.65
	-	✓	8.87	96.72	77.65	92.72
	✓	✓	6.56	98.40	93.08	93.86
CIFAR-100	-	-	62.66	73.11	30.05	75.73
	-	✓	26.75	91.59	68.27	71.29
	✓	✓	28.89	91.80	71.50	73.14

Table 2: Contribution of each regularization term of (3) on the OOD detection performance and the test accuracy of the DNN. Results are averaged over 10 runs and over 8 OOD datasets.

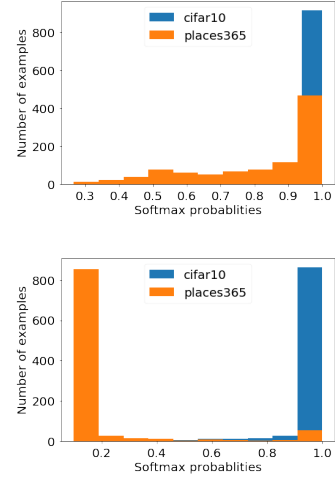


Figure 1: Histogram of softmax probabilities with CIFAR-10 as D_{in} and Places365 as D_{out}^{test} (1,000 samples from each dataset). *Top*: MSP baseline detector. *Bottom*: MSP detector fine-tuned with (3).

experiments, we incrementally added each regularization term to the loss function described by (3) and we measured its effect both in the OOD detection evaluation metrics as well as in the accuracy of the DNN on the test images of D_{in} . The results of these experiments validate that the combination of the two regularization terms of (3) not only improves the OOD detection performance of the DNN but also improves its accuracy on the test examples of D_{in} compared to the case where $\lambda_1 = 0$. Table 2 also demonstrates that our method can significantly improve the OOD detection performance of the DNN compared to the case where only the cross-entropy loss is minimized at the expense of only an insignificant degradation in the test accuracy of the DNN on examples generated by D_{in} .

4.1.3 TEXT CLASSIFICATION EXPERIMENTS

Results. The results of the text classification experiments are shown in Table 3. The detailed description of the text datasets used in the NLP OOD detection experiments is presented in Appendix B.1.

D_{in}	FPR90↓		AUROC↑		AUPR↑	
	+OE	OECC	+OE	OECC	+OE	OECC
20 Newsgroups	4.86	0.63	97.71	99.18	91.91	97.02
	0.78	0.75	99.28	99.32	97.64	97.52
	27.33	17.91	89.27	93.79	59.23	74.10

Table 3: NLP OOD example detection for the maximum softmax probability (MSP) baseline detector after fine-tuning with OE (Hendrycks et al., 2019) versus fine-tuning with OECC given by (3). All results are percentages and averaged over 10 runs and over 10 OOD datasets. Detailed experimental results are shown in Appendix B.3.

Network Architecture and Training Details. For all text classification experiments, similar to Hendrycks et al. (2019), we train 2-layer GRUs (Cho et al., 2014) for 5 epochs with learning rate 0.01 and a batch size of 64 and then we fine-tune them for 2 epochs using the OECC method described by (3). During fine-tuning, the WikiText-2 dataset was used as D_{out}^{OE} . The values of the hyperparameters λ_1 and λ_2 were chosen in the range [0.04, 0.1] using a separate validation dataset as described in Appendix B.2.

4.2 A COMBINATION OF OECC AND MAHALANOBIS DETECTION METHOD FOR OOD DETECTION

Lee et al. (2018b) proposed a post-training method for OOD detection that can be applied to any pre-trained softmax neural classifier. Under the assumption that the pre-trained features of a DNN can be fitted well by a class-conditional Gaussian distribution, they defined the confidence score using the Mahalanobis distance with respect to the closest class-conditional probability distribution, where its parameters are chosen as empirical class means and tied empirical covariance of training samples. To further distinguish in- and out-of-distribution examples, they proposed two additional techniques. In the first technique, they added a small perturbation before processing each input example to increase the confidence score of their method. In the second technique, they proposed a feature ensemble method in order to obtain a better calibrated score. The feature ensemble method extracts all the hidden features of the DNN and computes their empirical class mean and tied covariances. Subsequently, it calculates the Mahalanobis distance-based confidence score for each layer and finally calculates the weighted average of these scores by training a logistic regression detector using validation samples in order to calculate the weight of each layer at the final confidence score.

Since the Mahalanobis distance-based classifier proposed by Lee et al. (2018b) is a post-training method, it can be combined with the proposed OECC method described by (3). More specifically, in our experiments, we initially trained a DNN using the standard cross-entropy loss function and then we fine-tuned it with the OECC method given by (3). After fine-tuning, we applied the Mahalanobis distance-based classifier and we compared the obtained results against the results presented in Lee et al. (2018b). The simulation experiments on image classification tasks show that the combination of our method which is a training method, with the MD method which is a post-training method achieves superior results in the OOD detection task. A part of our experiments was based on the publicly available code of Lee et al. (2018b).

4.2.1 EVALUATION METRICS

To demonstrate the adaptability of our method, in these experiments, we adopt the OOD detection evaluation metrics used in Lee et al. (2018b).

- True Negative Rate at $N\%$ True Positive Rate (TNR_N): This performance metric measures the capability of an OOD detector to detect true negative examples when the true positive rate is set to 95%.

- Area Under the Receiver Operating Characteristic curve (AUROC): In the out-of-distribution detection task, the ROC curve (Davis & Goadrich, 2006) summarizes the performance of an OOD detection method for varying threshold values.
- Detection Accuracy (DAcc): As also mentioned in Lee et al. (2018b), this evaluation metric corresponds to the maximum classification probability over all possible thresholds ϵ :

$$1 - \min_{\epsilon} \{D_{in}(q(\mathbf{x}) \leq \epsilon)P(\mathbf{x} \text{ is from } D_{in}) + D_{out}(q(\mathbf{x}) > \epsilon)P(\mathbf{x} \text{ is from } D_{out})\},$$

where $q(\mathbf{x})$ is a confidence score. Similar to Lee et al. (2018b), we assume that $P(\mathbf{x} \text{ is from } D_{in}) = P(\mathbf{x} \text{ is from } D_{out})$.

4.2.2 EXPERIMENTAL SETUP

To demonstrate the adaptability and the effectiveness of our method, we adopt the experimental setup of Lee et al. (2018b). We train ResNet (He et al., 2016) with 34 layers using CIFAR-10, CIFAR-100 and SVHN datasets as D_{in} . For the CIFAR experiments, SVHN, TinyImageNet (a sample of 10,000 images drawn from the ImageNet dataset) and LSUN are used as D_{out}^{test} . For the SVHN experiments, CIFAR-10, TinyImageNet and LSUN are used as D_{out}^{test} . Both TinyImageNet and LSUN images are downsampled to 32×32 .

Similar to Lee et al. (2018b), for the MD method, we train the ResNet model for 200 epochs with batch size 128 by minimizing the cross-entropy loss using the SGD algorithm with momentum 0.9. The learning rate starts at 0.1 and is dropped by a factor of 10 at 50% and 75% of the training progress, respectively. Subsequently, we compute the Mahalanobis distance-based confidence score using both the input pre-processing and the feature ensemble techniques. The hyper-parameters that need to be tuned are the magnitude of the noise added at each test input example as well as the layer indexes for feature ensemble. Similar to Lee et al. (2018b), both of them are tuned using a separate validation dataset consisting of both in- and out-of-distribution data since the MD method originally requires access to OOD samples.

As mentioned earlier, since the Mahalanobis Detector (MD) is a post-training method for OOD detection, it can be combined with our proposed method. More specifically, we initially train the ResNet model with 34 layers for 200 epochs using exactly the same training setup as mentioned above. Subsequently, we fine-tune the network with the OECC method described by (3) using the 80 Million Tiny Images as D_{out}^{OE} . During fine-tuning, we use the SGD algorithm with momentum 0.9 and a cosine learning rate (Loshchilov & Hutter, 2017) with an initial value 0.001 using a batch size of 128 for data sampled from D_{in} and a batch size of 256 for data sampled from D_{out}^{OE} . For CIFAR-10 and 100 experiments, we fine-tuned the network for 30 and 20 epochs respectively, while for SVHN the corresponding number of epochs was 5. The values of the hyper-parameters λ_1 and λ_2 were chosen using a separate validation dataset consisting of both in- and out-of-distribution images similar to Lee et al. (2018b). The results are shown in Table 4.

D_{in}	D_{out}^{test}	TNR95↑		AUROC↑		DAcc↑	
		MD	OECC+MD	MD	OECC+MD	MD	OECC+MD
CIFAR-10	SVHN	96.4	97.3	99.1	99.2	95.8	96.3
	TinyImageNet	97.1	98.8	99.5	99.6	96.3	97.3
	LSUN	98.9	99.7	99.7	99.8	97.7	98.5
CIFAR-100	SVHN	91.9	93.0	98.4	98.7	93.7	94.2
	TinyImageNet	90.9	92.3	98.2	98.3	93.3	93.9
	LSUN	90.9	95.6	98.2	98.6	93.5	95.4
SVHN	CIFAR-10	98.4	99.9	99.3	99.9	96.9	99.2
	TinyImageNet	99.9	100.0	99.9	100.0	99.1	99.9
	LSUN	99.9	100.0	99.9	100.0	99.5	100.0

Table 4: Comparison using a ResNet-34 architecture between the Mahalanobis distance-based Detector (MD) (Lee et al., 2018b) and the combination of OECC with the MD method. The hyper-parameters are tuned using a validation dataset of in- and out-of-distribution data similar to Lee et al. (2018b).

4.3 A COMBINATION OF OECC AND GRAM MATRICES METHOD FOR OOD DETECTION

Sastry & Oore (2019) proposed a post-training method for OOD detection that does not require access to OOD data for hyper-parameter tuning as MD method (Lee et al., 2018b) does. More specifically, they proposed the use of higher order Gram matrices to compute pairwise feature correlations between the channels of each layer of a DNN. Subsequently, after computing the minimum and maximum values of the correlations for every class c that an example generated by D_{in} is classified, they used those values to calculate the layerwise deviation of each test sample, i.e. the deviation of test sample from the images seen during training with respect to each of the layers. Finally, they calculated the total deviation by taking a normalized sum of the layerwise deviations and using a threshold τ , they classified a sample as OOD if its corresponding total deviation was above the threshold. The experimental results presented in Sastry & Oore (2019) showed that GM method outperforms MD method in most of the experiments without requiring access to OOD samples to tune its parameters. However, it should be noted that GM, in its current form, does not perform equally well when the samples from D_{out}^{test} are close to D_{in} , as it happens for instance in the case where CIFAR-10 is used as D_{in} and CIFAR-100 is used as D_{out}^{test} .

ResNet experiments. For the results related to the GM method, we initially trained the ResNet model using exactly the same training details presented in Section 4.2.2 and then we applied the GM method where the tuning of the normalizing factor used to calculate the total deviation of a test image is done using a randomly selected validation partition from D_{in}^{test} as described in Sastry & Oore (2019). For the combined OECC+GM method, we initially trained the ResNet model as described above, then we fine-tuned it using the loss function described by (3) and finally, we applied the GM method. During fine-tuning, we used the SGD algorithm with momentum 0.9 and a cosine learning rate (Loshchilov & Hutter, 2017) with an initial value 0.001 using a batch size of 128 for data sampled from D_{in} and a batch size of 256 for data sampled from D_{out}^{OE} . In our experiments, the 80 Million Tiny Images dataset (Torralba et al., 2008) was considered as D_{out}^{OE} . For CIFAR-10 experiments, we fine-tuned the network for 30 epochs, for CIFAR-100 we fine-tuned it for 10, while for SVHN the corresponding number of epochs was 5. In contrast to the previous experiment where we combined the OECC method with the MD method, in this experiment, the hyper-parameters λ_1 and λ_2 of (3) were tuned using a separate validation dataset D_{out}^{val} . Note that D_{out}^{val} and D_{out}^{test} are disjoint. Therefore, for these experiments, no access to D_{out}^{test} was assumed. The results of the experiments are shown in Table 5.

D_{in}	D_{out}^{test}	TNR95↑		AUROC↑		DAcc↑	
		GM	OECC+GM	GM	OECC+GM	GM	OECC+GM
CIFAR-10	SVHN	97.6	99.2	99.4	99.7	96.7	98.0
	TinyImageNet	98.7	99.6	99.6	99.8	97.8	98.3
	LSUN	99.6	99.9	99.8	99.9	98.6	99.0
CIFAR-100	SVHN	81.4	87.2	96.2	97.1	89.8	91.9
	TinyImageNet	95.1	95.8	99.0	98.8	95.1	95.5
	LSUN	97.0	98.2	99.3	99.3	96.2	96.8
SVHN	CIFAR-10	85.7	98.3	97.3	99.3	91.9	96.9
	TinyImageNet	99.3	100.0	99.7	100.0	97.9	99.5
	LSUN	99.4	100.0	99.8	100.0	98.5	99.8

Table 5: Comparison using a ResNet-34 architecture between the GM method proposed by (Sastry & Oore, 2019) versus the combination of OECC method and the GM method. The tuning of the hyperparameters λ_1 and λ_2 of (3) is done using a separate validation dataset D_{out}^{val} . Note that D_{out}^{val} and D_{out}^{test} are disjoint, i.e. no access to OOD samples was assumed.

DenseNet experiments. For the results related to the GM method, we used the pre-trained DenseNet (Huang et al., 2017) model provided by Liang et al. (2018). The network has depth $L = 100$, growth rate $m = 12$ and dropout rate 0. It has been trained using the stochastic gradient descent algorithm with Nesterov momentum (Duchi et al., 2011; Kingma & Ba, 2014) for 300 epochs with batch size 64 and momentum 0.9. The learning rate started at 0.1 and was dropped by a factor of 10 at 50% and 75% of the training progress, respectively. Subsequently, we applied the GM method (Sastry & Oore, 2019) where the tuning of the normalizing factor used to calculate the total deviation of a test image was done using a randomly selected validation partition from D_{in}^{test} .

as described in Sastry & Oore (2019). For the combined OECC+GM method, we fine-tuned the pre-trained DenseNet network model provided by Liang et al. (2018) using the OECC loss function described by (3) and then we applied the GM method. During fine-tuning, we used the SGD algorithm with momentum 0.9 and a cosine learning rate (Loshchilov & Hutter, 2017) with an initial value 0.001 for CIFAR-10 and SVHN experiments and 0.01 for the CIFAR-100 experiments using a batch size of 128 for data sampled from D_{in} and a batch size of 256 for data sampled from D_{out}^{OE} . In our experiments, the 80 Million Tiny Images dataset (Torralba et al., 2008) was considered as D_{out}^{OE} . The DenseNet model was fine-tuned for 15 epochs for the CIFAR-10 experiments, for 10 epochs for the CIFAR-100 experiments, while for SVHN the corresponding number of epochs was 5. The hyperparameters λ_1 and λ_2 of the OECC method were tuned using a separate validation dataset D_{out}^{val} . Note that D_{out}^{val} and D_{out}^{test} are disjoint. The experimental results are presented in Table 6.

D_{in}	D_{out}^{test}	TNR95↑		AUROC↑		DAcc↑	
		GM	OECC+GM	GM	OECC+GM	GM	OECC+GM
CIFAR-10	SVHN	96.0	98.5	99.1	99.6	95.8	97.4
	TinyImageNet	98.8	99.3	99.7	99.8	97.9	98.3
	LSUN	99.5	99.8	99.9	99.9	97.9	99.0
CIFAR-100	SVHN	89.4	88.9	97.4	97.0	92.4	92.1
	TinyImageNet	95.8	96.2	99.0	99.0	95.6	95.7
	LSUN	97.3	98.1	99.4	99.3	96.4	97.0
SVHN	CIFAR-10	80.2	98.5	95.5	99.6	89.0	97.5
	TinyImageNet	99.1	99.9	99.7	100.0	97.9	99.7
	LSUN	99.5	100.0	99.8	100.0	98.5	99.9

Table 6: Comparison using a DenseNet-100 architecture between the GM method proposed by (Sastry & Oore, 2019) versus the combination of OECC method and the GM method. The tuning of the hyperparameters λ_1 and λ_2 of (3) is done using a separate validation dataset D_{out}^{val} . Note that D_{out}^{val} and D_{out}^{test} are disjoint, i.e. no access to OOD samples was assumed.

Discussion. The results presented in Table 4, Table 5 and Table 6 demonstrate the superior performance that can be achieved when combining training and post-training methods for OOD detection. More specifically, the MD method (Lee et al., 2018b) extracts the features from all layers of a pre-trained softmax neural classifier and then calculates the Mahalanobis distance-based confidence score. The GM method (Sastry & Oore, 2019) also extracts the features from a pre-trained softmax neural classifier and then computes higher order Gram matrices to subsequently calculate pairwise feature correlations between the channels of each layer of a DNN. As also mentioned earlier, both of these methods are post-training methods for OOD detection. On the other hand, the simulation results presented in Table 1, Table 2 and Table 3 showed that OECC, which belongs to the category of training methods for OOD detection, can teach the DNN to learn feature representations that can better distinguish in- and out-of distribution data compared to the baseline method (Hendrycks & Gimpel, 2017) and the OE method (Hendrycks et al., 2019). Therefore, by feeding a post-training method like the MD method (Lee et al., 2018b) or the GM method (Sastry & Oore, 2019) with better feature presentations, it is expected that one can achieve superior results in the OOD detection task as it is also validated by the experimental results in Table 4, Table 5 and Table 6.

5 CONCLUSION

In this paper, we proposed a novel method for OOD detection, called Outlier Exposure with Confidence Control (OECC). OECC includes two regularization terms the first of which minimizes the l_1 norm between the output distribution of the softmax layer of a DNN and the uniform distribution, while the second minimizes the Euclidean distance between the training accuracy of a DNN and its average confidence in its predictions on the training set. Experimental results showed that the proposed method achieves superior results in OOD detection with OE (Hendrycks et al., 2019) in both image and text classification tasks without requiring access to OOD samples. Additionally, we experimentally showed that our method can be combined with state-of-the-art post-training methods for OOD detection like the Mahalanobis Detector (MD) (Lee et al., 2018b) and the Gramian Matrices method (GM) (Sastry & Oore, 2019) demonstrating the desirability of combination of training and post-training methods for OOD detection in the future research efforts.

ACKNOWLEDGMENTS

We thank Google for donating Google Cloud Platform research credits used in this research.

REFERENCES

Vassileios Balntas, Edgar Riba, Daniel Ponsa, and Krystian Mikolajczyk. Learning local feature descriptors with triplets and shallow convolutional neural networks. In *Proceedings of the British Machine Vision Conference (BMVC)*, 2016.

Abhijit Bendale and Terrance Boult. Towards open world recognition. In *IEEE Conference on Computer Vision and Pattern Recognition (CVPR)*, 2015.

Petra Bevandić, Ivan Krešo, Marin Oršić, and Siniša Šegvić. Discriminative out-of-distribution detection for semantic segmentation. *arXiv preprint arXiv: 1808.07703*, 2018.

Samuel R. Bowman, Gabor Angeli, Christopher Potts, and Christopher D. Manning. A large annotated corpus for learning natural language inference. In *Proceedings of the 2015 Conference on Empirical Methods in Natural Language Processing (EMNLP)*, 2015.

Stephen Boyd and Lieven Vandenberghe. *Convex Optimization*. Cambridge University Press, 2004.

Kyunghyun Cho, Bart van Merriënboer, aglar Glehre, Dzmitry Bahdanau, Fethi Bougares, Holger Schwenk, and Yoshua Bengio. Learning phrase representations using rnn encoder-decoder for statistical machine translation. In *Empirical Methods in Natural Language Processing (EMNLP)*, 2014.

Mircea Cimpoi, Subhransu Maji, Iasonas Kokkinos, Sammy Mohamed, and Andrea Vedaldi. Describing textures in the wild. In *IEEE Conference on Computer Vision and Pattern Recognition (CVPR)*, 2014.

Jesse Davis and Mark Goadrich. The relationship between precision-recall and roc curves. In *International Conference on Machine Learning (ICML)*, 2006.

Michel Marie Deza and Elena Deza. *Encyclopedia of Distances*. Springer Berlin Heidelberg, 2009.

John Duchi, Elad Hazan, and Yoram Singer. Adaptive subgradient methods for online learning and stochastic optimization. *Journal of Machine Learning Research*, 12:2121–2159, 2011.

Desmond Elliott, Stella Frank, Khalil Sima’an, and Lucia Specia. Multi30K: Multilingual English-German Image Descriptions. *arXiv preprint arXiv: 1605.00459*, 2016.

Ian J. Goodfellow, Jean Pouget-Abadie, Mehdi Mirza, Bing Xu, David Warde-Farley, Sherjil Ozair, Aaron Courville, and Yoshua Bengio. Generative adversarial nets. In *International Conference on Neural Information Processing Systems (NIPS)*, pp. 2672–2680, 2014.

Chuan Guo, Geoff Pleiss, Yu Sun, and Kilian Q. Weinberger. On calibration of modern neural networks. In *International Conference on Machine Learning (ICML)*, 2017.

Trevor Hastie, Robert Tibshirani, and Jerome Friedman. *The Elements of Statistical Learning*. Springer Series in Statistics. Springer New York Inc., New York, NY, USA, 2001.

Kaiming He, Xiangyu Zhang, Shaoqing Ren, and Jian Sun. Deep residual learning for image recognition. In *IEEE Conference on Computer Vision and Pattern Recognition (CVPR)*, 2016.

Dan Hendrycks and Thomas G. Dietterich. Benchmarking Neural Network Robustness to Common Corruptions and Surface Variations. *arXiv preprint arXiv:1807.01697*, 2018.

Dan Hendrycks and Kevin Gimpel. A baseline for detecting misclassified and out-of-distribution examples in neural networks. *International Conference on Learning Representations (ICLR)*, 2017.

Dan Hendrycks, Mantas Mazeika, and Thomas Dietterich. Deep anomaly detection with outlier exposure. *International Conference on Learning Representations (ICLR)*, 2019.

Dan Hendrycks, Mantas Mazeika, Saurav Kadavath, and Dawn Song. Using self-supervised learning can improve model robustness and uncertainty. In *Neural Information Processing Systems (NeurIPS)*, 2019b.

Geoffrey Hinton, Oriol Vinyals, and Jeff Dean. Distilling the knowledge in a neural network. *arXiv preprint arXiv:1503.02531*, 2015.

Gao Huang, Zhuang Liu, Laurens van der Maaten, and Kilian Q Weinberger. Densely connected convolutional networks. In *Proceedings of the IEEE Conference on Computer Vision and Pattern Recognition (CVPR)*, 2017.

Diederik P Kingma and Jimmy Ba. Adam: A method for stochastic optimization. *arXiv preprint arXiv:1412.6980*, 2014.

Mark Kliger and Shachar Fleishman. Novelty Detection with GAN. *arXiv preprint arXiv:1802.10560*, 2018.

Alex Krizhevsky and Geoffrey Hinton. Learning multiple layers of features from tiny images. Technical report, University of Toronto, 2009.

Alex Krizhevsky, Ilya Sutskever, and Geoffrey E Hinton. Imagenet classification with deep convolutional neural networks. In *Advances in Neural Information Processing Systems 25*, pp. 1097–1105. 2012.

Vijay Kumar, Gustavo Carneiro, and Ian Reid. Learning Local Image Descriptors with Deep Siamese and Triplet Convolutional Networks by Minimising Global Loss Functions. In *IEEE Conference on Computer Vision and Pattern Recognition (CVPR)*, 2016.

Balaji Lakshminarayanan, Alexander Pritzel, and Charles Blundell. Simple and scalable predictive uncertainty estimation using deep ensembles. In *International Conference on Neural Information Processing Systems*, 2017.

Kimin Lee, Honglak Lee, Kibok Lee, and Jinwoo Shin. Training Confidence-calibrated Classifiers for Detecting Out-of-Distribution Samples. *International Conference on Learning Representations (ICLR)*, 2018a.

Kimin Lee, Kibok Lee, Honglak Lee, and Jinwoo Shin. A simple unified framework for detecting out-of-distribution samples and adversarial attacks. In *International Conference on Neural Information Processing Systems*, 2018b.

Shiyu Liang, Yixuan Li, and R. Srikant. Enhancing The Reliability of Out-of-distribution Image Detection in Neural Networks. *International Conference on Learning Representations (ICLR)*, 2018.

Si Liu, Risheek Garrepalli, Thomas G. Dietterich, Alan Fern, and Dan Hendrycks. Open Category Detection with PAC Guarantees. *arXiv preprint arXiv: 1808.00529*, 2018.

I. Loshchilov and F. Hutter. Sgdr: Stochastic gradient descent with warm restarts. In *International Conference on Learning Representations (ICLR)*, 2017.

Andrey Malinin and Mark Gales. Predictive uncertainty estimation via prior networks. In *Neural Information Processing Systems*, 2018.

Christopher D. Manning and Hinrich Schütze. *Foundations of Statistical Natural Language Processing*. MIT Press, 1999.

Sina Mohseni, Mandar Pitale, JBS Yadawa, and Zhangyang Wang. Self-supervised learning for generalizable out-of-distribution detection. In *Proceedings of the Thirty-Fourth AAAI Conference on Artificial Intelligence*, 2020.

Mahdi Pakdaman Naeini, Gregory F. Cooper, and Milos Hauskrecht. Obtaining well calibrated probabilities using bayesian binning. In *AAAI Conference on Artificial Intelligence*, 2015.

Yuval Netzer, Tao Wang, Adam Coates, Alessandro Bissacco, Bo Wu, and Andrew Y. Ng. Reading digits in natural images with unsupervised feature learning. In *NIPS Workshop on Deep Learning and Unsupervised Feature Learning 2011*, 2011.

Anh Mai Nguyen, Jason Yosinski, and Jeff Clune. Deep neural networks are easily fooled: High confidence predictions for unrecognizable images. In *IEEE Conference on Computer Vision and Pattern Recognition (CVPR)*, pp. 427–436, 2015.

Gabriel Pereyra, George Tucker, Jan Chorowski, Lukasz Kaiser, and Geoffrey E. Hinton. Regularizing neural networks by penalizing confident output distributions. In *International Conference on Learning Representations (ICLR)*, 2017.

J. Platt. Probabilistic outputs for support vector machines and comparison to regularized likelihood methods. In *Advances in Large Margin Classifiers*, 1999.

Chandramouli Shama Sastry and Sageev Oore. Detecting out-of-distribution examples with in-distribution examples and gram matrices. *arXiv preprint arXiv:1912.12510*, 2019.

Richard Socher, Alex Perelygin, Jean Y. Wu, Jason Chuang, Christopher D. Manning, Andrew Y. Ng, and Christopher Potts. Recursive deep models for semantic compositionality over a sentiment treebank. In *Conference on empirical methods in natural language processing (EMNLP)*, 2013.

Christian Szegedy, Vincent Vanhoucke, Sergey Ioffe, Jonathon Shlens, and Zbigniew Wojna. Rethinking the inception architecture for computer vision. *arXiv preprint arXiv: 1512.00567*, 2015.

Antonio Torralba, Rob Fergus, and William T. Freeman. 80 million tiny images: A large data set for nonparametric object and scene recognition. *IEEE Transactions on Pattern Analysis and Machine Intelligence*, 30(11), 2008.

Fisher Yu, Yinda Zhang, Shuran Song, Ari Seff, and Jianxiong Xiao. Lsun: Construction of a large-scale image dataset using deep learning with humans in the loop. *arXiv preprint arXiv:1506.03365*, 2015.

Yang Yu, Wei-Yang Qu, Nan Li, and Zimin Guo. Open-Category Classification by Adversarial Sample Generation. *arXiv preprint arXiv: 1705.08722*, 2017.

Sergey Zagoruyko and Nikos Komodakis. Wide residual networks. In *British Machine Vision Conference (BMVC)*, 2016.

B. Zhou, A. Lapedriza, A. Khosla, A. Oliva, and A. Torralba. Places: A 10 million image database for scene recognition. *IEEE Transactions on Pattern Analysis and Machine Intelligence*, 40(06): 1452–1464, 2018.

A EXPANDED IMAGE OOD DETECTION RESULTS AND DATASETS USED FOR COMPARISON WITH STATE-OF-THE-ART IN OE

A.1 IMAGE OOD DETECTION RESULTS

D_{in}	D_{out}^{test}	FPR95↓		AUROC↑		AUPR↑	
		+OE	OECC	+OE	OECC	+OE	OECC
SVHN	Gaussian	0.0	0.0	100.	100.	100.	99.4
	Bernulli	0.0	0.0	100.	100.	100.	99.2
	Blobs	0.0	0.0	100.	100.	100.	99.6
	Icons-50	0.3	0.1	99.8	99.9	99.2	99.5
	Textures	0.2	0.1	100.	100.	99.7	99.6
	Places365	0.1	0.0	100.	100.	99.9	99.7
	LSUN	0.1	0.0	100.	100.	99.9	99.7
	CIFAR-10	0.1	0.0	100.	100.	99.9	99.7
Mean		0.10	0.03	99.98	99.99	99.83	99.55
CIFAR-10	Gaussian	0.7	0.7	99.6	99.8	94.3	99.0
	Rademacher	0.5	1.1	99.8	99.6	97.4	97.6
	Blobs	0.6	1.5	99.8	99.1	98.9	91.7
	Textures	12.2	4.0	97.7	98.9	91.0	95.0
	SVHN	4.8	1.4	98.4	99.6	89.4	97.9
	Places365	17.3	13.3	96.2	96.9	87.3	89.5
	LSUN	12.1	6.7	97.6	98.4	89.4	91.9
	CIFAR-100	28.0	23.8	93.3	94.9	76.2	82.0
Mean		9.50	6.56	97.81	98.40	90.48	93.08
CIFAR-100	Gaussian	12.1	0.7	95.7	99.7	71.1	97.2
	Rademacher	17.1	0.7	93.0	99.7	56.9	96.2
	Blobs	12.1	1.3	97.2	99.6	86.2	96.3
	Textures	54.4	50.1	84.8	87.8	56.3	61.5
	SVHN	42.9	16.7	86.9	94.9	52.9	74.1
	Places365	49.8	47.8	86.5	88.1	57.9	58.5
	LSUN	57.5	56.6	83.4	85.9	51.4	53.0
	CIFAR-10	62.1	57.2	75.7	78.7	32.6	35.2
Mean		38.50	28.89	87.89	91.80	58.15	71.50

Table 7: Image OOD example detection for the maximum softmax probability (MSP) baseline detector after fine-tuning with OE (Hendrycks et al., 2019) versus fine-tuning with OECC given by (3). All results are percentages and averaged over 10 runs. Values are rounded to the first decimal digit. As also mentioned before, for these results, no access to OOD samples was assumed.

A.2 D_{in} , D_{out}^{OE} AND D_{out}^{test} FOR IMAGE EXPERIMENTS

SVHN: The Street View House Number (SVHN) dataset (Netzer et al., 2011) consists of 32×32 color images out of which 604,388 are used for training and 26,032 are used for testing. The dataset has 10 classes and was collected from real Google Street View images. Similar to Hendrycks et al. (2019), we rescale the pixels of the images to be in $[0, 1]$.

CIFAR 10: This dataset (Krizhevsky & Hinton, 2009) contains 10 classes and consists of 60,000 32×32 color images out of which 50,000 belong to the training and 10,000 belong to the test set. Before training, we standardize the images per channel similar to Hendrycks et al. (2019).

CIFAR 100: This dataset (Krizhevsky & Hinton, 2009) consists of 20 distinct superclasses each of which contains 5 different classes giving us a total of 100 classes. The total number of images in the dataset are 60,000 and we use the standard 50,000/10,000 train/test split. Before training, we standardize the images per channel similar to Hendrycks et al. (2019).

80 Million Tiny Images: The 80 Million Tiny Images dataset (Torralba et al., 2008) was exclusively used in our experiments in order to represent D_{out}^{OE} . It consists of 32×32 color images collected from the Internet. Similar to Hendrycks et al. (2019), in order to make sure that D_{out}^{OE} and D_{out}^{test} are

disjoint, we removed all the images of the dataset that appear on CIFAR 10 and CIFAR 100 datasets.

Places365: Places365 dataset introduced by Zhou et al. (2018) was exclusively used in our experiments in order to represent D_{out}^{test} . It consists of millions of photographs of scenes.

Gaussian: A synthetic image dataset created by i.i.d. sampling from an isotropic Gaussian distribution.

Bernoulli: A synthetic image dataset created by sampling from a Bernoulli distribution.

Blobs: A synthetic dataset of images with definite edges.

Icons-50: This dataset introduced by Hendrycks & Dietterich (2018) consists of 10,000 images belonging to 50 classes of icons. As part of preprocessing, we removed the class “Number” in order to make it disjoint from the SVHN dataset.

Textures: This dataset contains 5,640 textural images (Cimpoi et al., 2014).

LSUN: It consists of around 1 million large-scale images of scenes (Yu et al., 2015).

Rademacher: A synthetic image dataset created by sampling from a symmetric Rademacher distribution.

A.3 VALIDATION DATA FOR IMAGE EXPERIMENTS

Uniform Noise: A synthetic image dataset where each pixel is sampled from $\mathcal{U}[0, 1]$ or $\mathcal{U}[-1, 1]$ depending on the input space of the classifier.

Arithmetic Mean: A synthetic image dataset created by randomly sampling a pair of in-distribution images and subsequently taking their pixelwise arithmetic mean.

Geometric Mean: A synthetic image dataset created by randomly sampling a pair of in-distribution images and subsequently taking their pixelwise geometric mean.

Jigsaw: A synthetic image dataset created by partitioning an image sampled from D_{in} into 16 equally sized patches and by subsequently permuting those patches.

Speckle Noised: A synthetic image dataset created by applying speckle noise to images sampled from D_{in} .

Inverted Images: A synthetic image dataset created by shifting and reordering the color channels of images sampled from D_{in} .

RGB Ghosted: A synthetic image dataset created by inverting the color channels of images sampled from D_{in} .

B EXPANDED TEXT OOD DETECTION RESULTS AND DATASETS USED FOR COMPARISON WITH STATE-OF-THE-ART IN OE

B.1 D_{in} , D_{out}^{OE} AND D_{out}^{test} FOR NLP EXPERIMENTS

20 Newsgroups: This dataset contains 20 different newsgroups, each corresponding to a specific topic. It contains around 19,000 examples and we used the standard 60/40 train/test split.

TREC: A question classification dataset containing around 6,000 examples from 50 different classes. Similar to Hendrycks et al. (2019), we used 500 examples for the test phase and the rest for training.

SST: The Stanford Sentiment Treebank (Socher et al., 2013) is a binary classification dataset for sentiment prediction of movie reviews containing around 10,000 examples.

WikiText-2: This dataset contains over 2 million articles from Wikipedia and is exclusively used as D_{out}^{OE} in our experiments. We used the same preprocessing as in Hendrycks et al. (2019) in order to have a valid comparison.

SNLI: The Stanford Natural Language Inference (SNLI) corpus is a collection of 570,000 human-written English sentence pairs (Bowman et al., 2015).

IMDB: A sentiment classification dataset containing movies reviews.

Multi30K: A dataset of English and German descriptions of images (Elliott et al., 2016). For our experiments, only the English descriptions were used.

WMT16: A dataset used for machine translation tasks. For our experiments, only the English part of the test set was used.

Yelp: A dataset containing reviews of users for businesses on Yelp.

EWT: The English Web Treebank (EWT) consists of 5 different datasets: weblogs (EWT-W), newsgroups (EWT-N), emails (EWT-E), reviews (EWT-R) and questions-answers (EWT-A).

B.2 VALIDATION DATA FOR NLP EXPERIMENTS

The validation dataset D_{out}^{val} used for the NLP OOD detection experiments was constructed as follows. For each D_{in} dataset used, we used the rest two in-distribution datasets as D_{out}^{val} . For instance, during the experiments where *20 Newsgroups* represented D_{in} , we used *TREC* and *SST* as D_{out}^{val} making sure that D_{out}^{val} and D_{out}^{test} are disjoint.

B.3 TEXT OOD DETECTION RESULTS

D_{in}	D_{out}^{test}	FPR90↓		AUROC↑		AUPR↑	
		+OE	OECC	+OE	OECC	+OE	OECC
20 Newsgroups	SNLI	12.5	2.1	95.1	97.1	86.3	93.0
	IMDB	18.6	2.5	93.5	98.2	74.5	92.9
	Multi30K	3.2	0.1	97.3	99.4	93.7	98.6
	WMT16	2.0	0.2	98.8	99.8	96.1	99.4
	Yelp	3.9	0.4	97.8	99.6	87.9	97.9
	EWT-A	1.2	0.2	99.2	99.8	97.3	98.4
	EWT-E	1.4	0.1	99.2	99.9	97.2	98.9
	EWT-N	1.8	0.5	98.7	99.2	95.7	94.5
	EWT-R	1.7	0.1	98.9	99.4	96.6	98.3
	EWT-W	2.4	0.1	98.5	99.4	93.8	98.3
Mean		4.86	0.63	97.71	99.18	91.91	97.02
TREC	SNLI	4.2	0.8	98.1	99.1	91.6	94.9
	IMDB	0.6	0.6	99.4	98.9	97.8	97.1
	Multi30K	0.3	0.2	99.7	99.9	99.0	99.6
	WMT16	0.2	0.2	99.8	99.9	99.4	99.6
	Yelp	0.4	0.8	99.7	99.1	96.1	92.9
	EWT-A	0.9	4.0	97.7	98.0	96.1	95.6
	EWT-E	0.4	0.3	99.5	99.2	99.1	98.1
	EWT-N	0.3	0.2	99.6	99.9	99.2	99.6
	EWT-R	0.4	0.2	99.5	99.6	98.8	98.9
	EWT-W	0.2	0.2	99.7	99.6	99.4	98.9
Mean		0.78	0.75	99.28	99.32	97.64	97.52
SST	SNLI	33.4	7.4	86.8	95.8	52.0	76.4
	IMDB	32.6	10.8	85.9	95.8	51.5	77.6
	Multi30K	33.0	5.1	88.3	97.9	58.9	86.9
	WMT16	17.1	3.6	92.9	98.3	68.8	88.1
	Yelp	11.3	15.6	92.7	95.2	60.0	81.1
	EWT-A	33.6	21.4	87.2	92.7	53.8	70.8
	EWT-E	26.5	22.6	90.4	92.4	63.7	67.7
	EWT-N	27.2	19.2	90.1	93.6	62.0	67.4
	EWT-R	41.4	36.7	85.6	88.1	54.7	62.5
	EWT-W	17.2	36.7	92.8	88.1	66.9	62.5
Mean		27.33	17.91	89.27	93.79	59.23	74.10

Table 8: NLP OOD example detection for the maximum softmax probability (MSP) baseline detector after fine-tuning with OE (Hendrycks et al., 2019) versus fine-tuning with OECC given by (3). All results are percentages and the result of 10 runs. Values are rounded to the first decimal digit. As also mentioned before, for these results, no access to OOD samples was assumed.

C CALIBRATION EXPERIMENTS

Guo et al. (2017) discovered that deep neural networks are not well calibrated. In their initial experiment, they observed that a deep neural network like a 110-layer ResNet (He et al., 2016) has an average confidence on its predictions for CIFAR-100 images which is much higher than its accuracy.

As discussed earlier in Section 3 and as was also shown experimentally, the purpose of the second term of the loss function described by (3) is to further distinguish in- and out-of-distribution examples and enhance the OOD detection capability of a neural network by pushing the maximum prediction probabilities produced by the softmax layer for the in-distribution examples to a higher level. Motivated by the fact that overconfident predictions constitute a symptom of overfitting (Szegedy et al., 2015) and also by the results of the experiment of (Guo et al., 2017), we expect that by minimizing the squared distance between the training accuracy of the DNN and the average confidence in its predictions for examples drawn from D_{in} , not only will the neural network have a higher OOD detection capability but it will also be more calibrated.

To validate our hypothesis, we use two miscalibration measures, namely the Expected Calibration Error (ECE) and the Maximum Calibration Error (MCE) (Naeini et al., 2015). ECE measures the difference in expectation between confidence and accuracy while MCE measures the worst-case deviation between confidence and accuracy.

To evaluate our method, we draw 1000 test samples from D_{in} and we compare the miscalibration errors for the MSP baseline detector and the MSP detector fine-tuned with the OECC method described by (3). We observe that the minimization of the squared distance between the average confidence of the neural network and its training accuracy through the second term of (3) also generalizes to the test set by reducing the miscalibration errors for both image and text datasets. As an example, in Figure 2, we plot the miscalibration errors considering as D_{in} the CIFAR-100 and the SST datasets respectively.

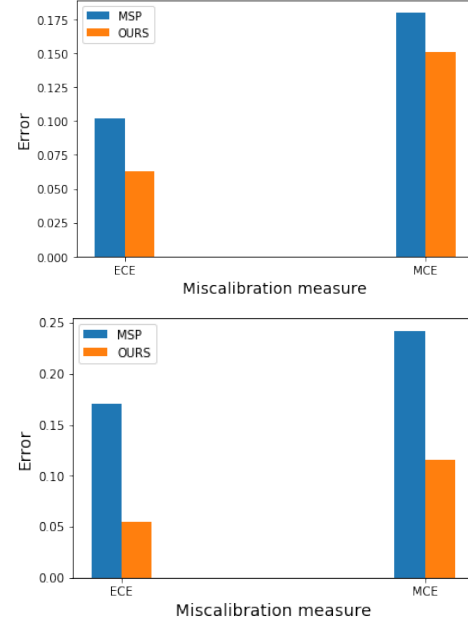


Figure 2: ECE and MCE for the MSP baseline detector and for the MSP baseline detector after fine-tuning with the OECC method described by (3). *Top:* CIFAR-100. *Bottom:* SST.